



# Seasonal and inter-annual variability of the quasi 2 day wave over Collm (51.3° N, 13° E) as obtained from VHF meteor radar measurements

F. Lilienthal and Ch. Jacobi

Institute for Meteorology, University of Leipzig, Stephanstr. 3, 04103 Leipzig, Germany

Correspondence to: F. Lilienthal (friederike.lilienthal@uni-leipzig.de)

Received: 18 December 2013 – Revised: 31 January 2014 – Accepted: 17 February 2014 – Published: 10 November 2014

**Abstract.** The quasi 2 day wave (QTDW) over Collm (51° N, 13° E) has been studied between September 2004 and September 2013 using a VHF meteor radar. The 9 year mean amplitudes show a strong summer maximum with several irregular bursts and much weaker winter maxima. In summer, the meridional amplitude is slightly larger than the zonal one with about  $15 \text{ m s}^{-1}$  at 91 km height. Phase differences are slightly higher than  $90^\circ$ , which indicates a polarization that is nearly circular. On an average the QTDW is amplified after a maximum of zonal wind shear. This can be realized in the summer mesospheric jet where the zonal wind component has its minimum or, in other words, the easterly jet maximizes. Thus, instability is found as a likely forcing mechanism. QTDW amplitudes exhibit considerable inter-annual variability. In particular, there is a possible relation between the QTDW amplitude and the 11-year solar cycle in winter but not in summer.

## 1 Introduction

The quasi 2 day wave (QTDW) is one of the most striking dynamical features in the mesosphere and lower thermosphere. It is characterized by a strong amplification during summer at low and mid-latitudes. At high latitudes it shows a different behavior, e.g. with maxima during winter (Nozawa et al., 2003; Muller and Nelson, 1978). The QTDW has been frequently observed by ground based (e.g., Muller, 1972; Babadshyanov et al., 1973; Plumb et al., 1987; Jacobi et al., 1997; Gurubaran et al., 2001; Pancheva, 2006) and satellite instruments (Wu et al., 1996; Bristow et al., 1999). Additionally, several numerical studies simulated possible excitation processes (Salby, 1981a, b; Plumb, 1983; Palo et al., 1999;

Salby and Callaghan, 2001; Merzlyakov and Jacobi, 2004). The QTDW was first reported by Muller (1972) using a meteor wind radar over Sheffield. He explored significant oscillations with a period near 51 h. Salby (1981a, b) suggested the QTDW to be a manifestation of a Rossby gravity normal mode in an isothermal windless atmosphere with wave number 3 but could not explain its burst-like behavior. Applying a one-dimensional stability analysis Plumb (1983) introduced baroclinic instability as an excitation mechanism. Pfister (1985) supported this theory by a two-dimensional quasi-geostrophic model and found a QTDW with wave numbers 2–4 and maxima at middle and high latitudes. However, this result did not resemble all the characteristics of the wave. Hence, Salby and Callaghan (2001) combined both mechanisms in a numerical model resulting in an excitation in the winter hemisphere by planetary wave activities. Crossing the equator to the summer hemisphere the QTDW is then enhanced by easterly baroclinic instability (Wu et al., 1996). A hemispheric asymmetry has been observed (e.g., Tsuda et al., 1988; Tunbridge et al., 2011) with stronger amplitudes in the Southern Hemisphere (SH) compared to Northern Hemisphere (NH). The meridional component tends to be slightly larger than the zonal one at mid-latitudes (Pancheva et al., 2004) or of similar magnitude (Jacobi et al., 2001). The period of approximately 2 days varies between 43–56 h in the NH (Pancheva et al., 2004). Generally, they can be divided into three groups as suggested by Malinga and Ruohoniemi (2007). The dominating one has periods close to 48 h with wave numbers 2 (Tunbridge et al., 2011) and 3 (Malinga and Ruohoniemi, 2007; Tunbridge et al., 2011; Pancheva et al., 2004). The second group has much shorter periods of about 42–43 h. Different wave numbers are reported such as 2 and 3 (Malinga and Ruohoniemi, 2007) or 4 (Tunbridge et al.,

2011; Pancheva et al., 2004). The last group covers periods longer than 48 h and peaks at 52 h with wave numbers 2 and 3 (Malinga and Ruohoniemi, 2007; Tunbridge et al., 2011; Pancheva et al., 2004). In the SH these three groups could not be observed and periods are close to 48 h with wave number 3 (Wu et al., 1996). Craig and Elford (1981) explored phase locking relative to the sun and suggested nonlinear interactions with diurnal tides. A correlation of QTDW amplitudes with the 11-year solar cycle has been found by Jacobi et al. (1997), who explained this finding by a stronger mesospheric wind shear during solar maximum.

A local climatology of QTDW amplitudes and phases over Collm as seen by ground-based radio measurements in the low-frequency (LF) range is already available (Jacobi et al., 1997). However, their results base on measurements with regular daily data gaps, which may affect wave analysis and lead to uncertainties of amplitude and phase detection. By analyzing new meteor radar wind data 2004–2013 from Collm further information about the mid-latitude QTDW could be provided with greater accuracy than the earlier LF measurements, and using time intervals comparable to those of global satellite data. Background shear is used as a proxy for instability as suggested by Merzlyakov and Jacobi (2004) in a numerical work.

## 2 Description of measurements and data analysis

A SKiYMET VHF meteor radar (MR) is operated at Collm Observatory (51° N, 13° E) since late summer 2004 to measure mesopause region winds, temperatures, and meteor parameters, replacing earlier LF drift measurements (e.g., Jacobi et al., 1997). The climatology of background winds and tides as measured by this radar was presented by Jacobi (2012). The radar uses the Doppler shift of the reflected VHF radio wave from ionized meteor trails giving the radial velocity along the line of sight of the radio wave. It operates at 36.2 MHz and has a pulse repetition frequency of 2144 Hz which is effectively reduced to 536 Hz due to a 4-point coherent integration. The power of the radar is 6 kW. The transmitting antenna is a 3-element Yagi with a sampling resolution of 1.87 ms and an angular and range resolution of about 2° and 2 km, respectively. The receiving interferometer consists of five 2-element Yagi antennas arranged as an asymmetric cross. This allows to calculate azimuth and elevation angle from phase comparisons of the individual receiver antenna pairs. Together with range measurements the meteor trail position is detected. The radar and data collection procedure is described in detail by Hocking et al. (2001).

The meteor trail reflection heights vary between 75 and 110 km with a maximum around 90 km (e.g., Stober et al., 2008). To analyze the wind field, the received meteors and corresponding radial winds are binned in six height gates centered at 82, 85, 88, 91 and 98 km. However, Jacobi (2012) found that nominal and mean heights are not necessarily the

same owing to the vertical distribution of meteor count rates that decrease with altitude above 90 km. Thus, the uppermost height gate with a nominal height of 98 km refers to a mean height of about 97 km. The radar measurements deliver half-hourly mean horizontal wind values that are calculated by a least squares fit of the horizontal half-hourly wind components to the individual radial wind while vertical winds are assumed to be small (Hocking et al., 2001). An outlier rejection is added.

The earlier LF spaced receiver method that has been applied at Collm since the late 1950s until 2007 was based on the reflection of commercial LF radio waves in the lower ionospheric E region. This led to regular daily gaps due to increased absorption during daylight hours, particularly long in summer. These measurements have been used earlier to obtain a QTDW climatology over Collm (Jacobi et al., 1997). However, the limitations of the LF method may give rise to potential artifacts, namely uncertainties of the amplitude, and possible effects on the analyzed phases. Therefore, here the MR winds are analyzed and can be used to evaluate the earlier results.

To obtain the amplitudes and phases of the QTDW a harmonic analysis has been applied based on a least-squares fit of the prevailing wind, tidal oscillations, and a period of exactly 48 h. Each individual fit is based on 11 days of half-hourly mean winds and the results are attributed to the center of this data window. The window was then shifted by one day. The procedure was performed for both the zonal and the meridional wind component, and for each height gate separately. The following results are based on these data. Note that the real period of the QTDW may slightly differ from 48 h, so that actually we defined a proxy for the QTDW only, and do not present the real amplitudes themselves. However, Malinga and Ruohoniemi (2007) found that the group of QTDWs with periods close to 48 h dominates. This is in agreement with the results of Jacobi et al. (1997) who showed that the resulting error of the amplitudes and phases for a period of 48 h with respect to the true values is small.

## 3 Results

### 3.1 Climatology of the QTDW over Collm

Wind data at 91 km measured from September 2004 to September 2013 have been used to present nine year mean amplitudes of the QTDW as shown in Fig. 1. Additionally the vertical wind shear components were calculated as the vertical zonal and meridional prevailing wind gradients taken from the difference of prevailing winds at both adjacent height gates. In this plot zonal amplitude  $u$  and meridional amplitude  $v$  of the wave are combined in a total amplitude:

$$v_{\text{tot}} = \sqrt{u^2 + v^2}.$$

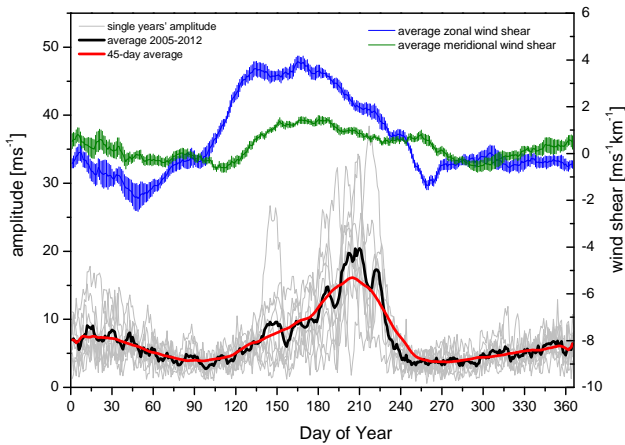


**Figure 1.** Total annual amplitudes 2004–2013 (light gray), average value of the years 2004–2013 (black) and 45 day adjacent average (red). The upper blue and green curves denote the zonal and meridional wind shear, respectively, including standard error. Data refer to a height of 91 km.

In Fig. 1, the seasonal cycle of QTDW amplitudes is shown. The heavy black line in the lower part shows the nine year mean amplitude and the red line shows a 45-point averaging of the mean. Due to the fact that the QTDW occurs as short bursts at different times in different years, the black and red lines in Fig. 1 do not show a typical evolution of the QTDW during one given year, but rather a long-term mean which may strongly differ from the amplitudes in a single year. To visualize this, and to give an impression of the inter-annual variability of the QTDW bursts, the amplitudes of single years are shown as light gray lines. On an average, four irregular bursts are found in summer. One is found at the end of May, three others are situated very close to each other in July and August. But having a closer look to the single years we notice the first maximum owing to very large amplitudes in one single year (2006) only. In a smoothed annual cycle (red), the May peak is averaged out and left is a clear maximum in July of about  $15 \text{ m s}^{-1}$ . The amplitude starts to increase in May and decreases until late August with a value of  $5 \text{ m s}^{-1}$  during the rest of the year, apart from a weak secondary winter maximum that already has been described in the literature by Muller and Nelson (1978). The vertical zonal shear in Fig. 1 shows a maximum when the amplitude of the wave starts to increase. This holds for summer QTDW. The winter wave does not seem to be related to shear.

In the following we report some features of the summer QTDW as seen by the radar. Figure 2 shows the phase differences between the zonal and meridional components for total amplitudes larger than  $15 \text{ m s}^{-1}$ . The difference between white bars (for whole year) and black bars (for summer only), represented by the remaining visible white part, only covers 10 of 266 events. This is due to the fact that large amplitudes only appear in summer when the QTDW amplifies.

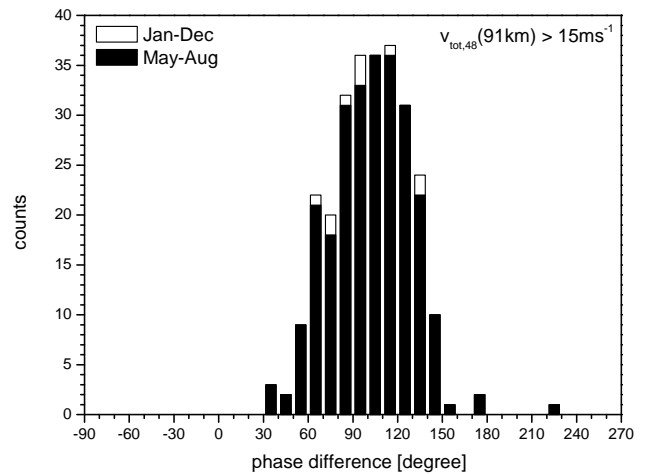


**Figure 2.** Histogram of the 91 km (gate 4) phase differences of zonal and meridional component for amplitudes larger than  $15 \text{ m s}^{-1}$ . White bars: whole year (January–December) data, 266 events. Black bars: summer (May–August) data, 256 events.

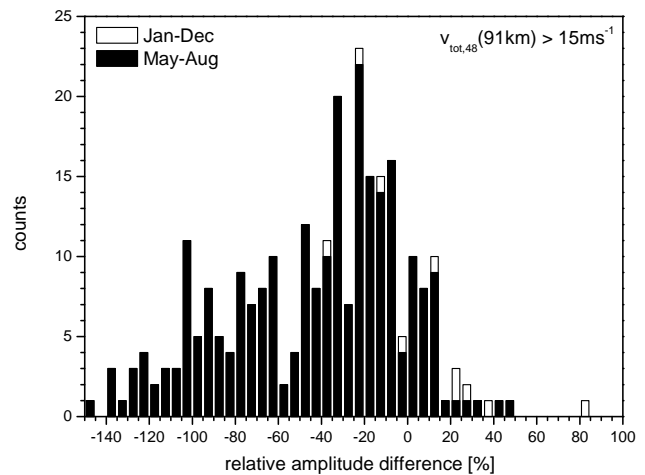


**Figure 3.** Histogram of the 91 km (gate 4) relative amplitude differences  $\Delta v$  of zonal and meridional component for amplitudes larger than  $15 \text{ m s}^{-1}$ . White bars: whole year (January–December) data, 266 events. Black bars: summer (May–August) data, 256 events. Positive values denote larger zonal than meridional amplitudes.

Phase differences of the wave accumulate at slightly more than  $90^\circ$ . For small amplitudes (not shown here), phase differences are more or less randomly distributed between 0 and  $360^\circ$ . This means that these results essentially do not refer to waves, but mainly to more irregular day-to-day fluctuations.

Figure 3 shows the relative amplitude difference of the zonal and meridional components:

$$\frac{v_{48,z} - v_{48,m}}{v_{48}} = 2 \frac{v_{48,z} - v_{48,m}}{v_{48,z} + v_{48,m}} \quad (1)$$

As can be seen from Fig. 3 the meridional component is larger than the zonal component, which has been reported

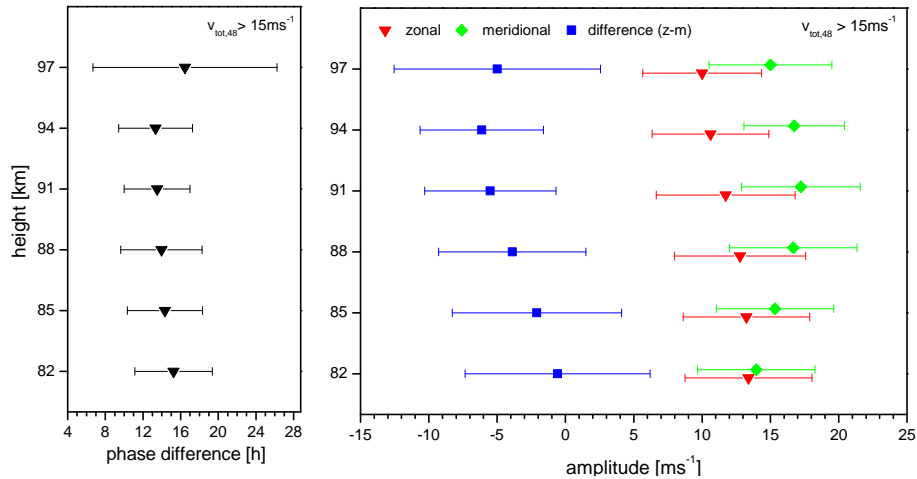


**Figure 4.** Left panel: mean phase difference (black) between zonal and meridional component 2004–2013 with standard deviation. Right panel: zonal (red) and meridional (green) mean amplitude 2004–2013 with standard deviation. Amplitude difference with standard deviation in blue. For both panels only dates with total amplitude  $> 15 \text{ m s}^{-1}$  are used.

in the literature (Pancheva et al., 2004) but was not seen in the earlier LF measurements by Jacobi et al. (1997, 2001).

Figure 4 shows the mean phase difference between zonal and meridional component as well as the amplitude in each component and their differences for all six height gates. Again, chosen are only events with total amplitude  $v_{\text{tot}} > 15 \text{ m s}^{-1}$ . These high amplitudes are only reached in summer when the QTDW amplifies after Fig. 2. The amplitude difference slightly changes with altitude. The zonal and meridional QTDW amplitudes are nearly the same at 82 km. At the upper height gates the meridional component is slightly larger than the zonal one. Note that the difference between zonal and meridional amplitude is dependent on the meridional structure of the wave which may vary from year to year. Phase differences are slightly greater than 12 h ( $90^\circ$ ) and do not change with altitude.

### 3.2 Connection between QTDW amplitude and wind shear

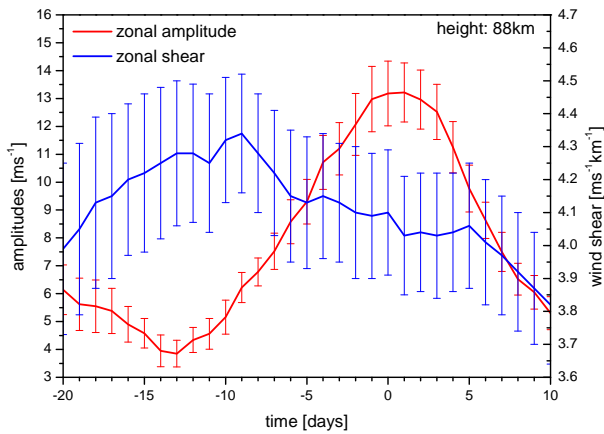
Charney and Stern (1962) stated that the northward gradient of the quasi-geostrophic potential vorticity  $q_y$  must change sign to enable baroclinic instability. This is possible in the vicinity of the summer mesospheric jet where the zonal wind component has a minimum (maximum easterly winds). The strongest winds of the mesospheric jet are located at lower altitudes and are therefore not seen by radar, but we may use the vertical wind shear above as a coarse proxy for the strength of the jet.

Figure 1 already suggests a relation between vertical wind shear of the zonal wind and QTDW amplification. To analyze this in more detail, a superposed epoch analysis of wind shears during strong QTDW events was used. Key events are represented by amplitude maxima that are determined from

the low-pass filtered time series in order to find only significant maxima. This day of maximum QTDW amplitude in the low-pass filter was further set to zero time. In a window of 30 days ( $-20$  to  $+10$  days) all events were averaged in amplitude and wind shear of the real time series. The results are shown in Fig. 5. As the position of a maximum of the low pass filter is not necessarily exactly identical with the one of the unfiltered amplitude the maximum of the average amplitude over all events is not exactly at zero time. However, as suggested by Fig. 1 we can also see the connection between shear and amplitude in this plot. The amplitude starts to increase when the shear reaches its maximum. This is in agreement with results presented by Pendlebury (2012) and Ern et al. (2013), who found that QTDW activity maximizes somewhat later than the peak winds of the mesospheric jet. We find maximum QTDW amplitudes on an average 10 days after maximum wind shear. The decreasing tendency for the wind shear during the QTDW events suggests that the wave acts to diminish the source of instability, i.e., the wind shear (see also Merzlyakov and Jacobi, 2004). This is in coincidence with the results obtained by Pendlebury (2012) and Ern et al. (2013) who found that the forcing of the QTDW is opposite to the wind direction in the jet.

### 3.3 Inter-annual variability

Earlier analyses have shown considerable inter-annual variability of QTDW bursts already. In particular, a decadal variability in phase with the 11 year solar cycle was suggested by Jacobi et al. (1997). An overview of the inter-annual variability of the seasonal mean QTDW amplitudes as seen by the Collm meteor radar is given in Fig. 6, separately for summer (May–August) and winter (November–February) means. The total amplitude for different gates, indicated by different



**Figure 5.** Epoch analysis of zonal amplitude (red) and vertical shear of the zonal wind (blue) using a 30 day window. Error bars indicate standard error.

colors, behave similarly. Additionally to the amplitudes of the QTDW the F10.7 solar radio fluxes not corrected for Sun-Earth distance are plotted as a proxy for solar activity. In winter we note a possible connection between QTDW amplitudes and solar flux. The correlation coefficient has been calculated from the 4-monthly mean total amplitudes. The maximum of the correlation coefficient in winter between the second and the fifth gate is  $r = 0.80$  at 85 km height. During summer, the correlation is much weaker and mainly negative with the strongest value of  $r = -0.43$  at 85 km height and weaker values above.

**4 Discussion and conclusion**

The QTDW has been analyzed using 9 years of wind data of the Collm VHF meteor radar that replaced earlier LF measurements in 2004. Strong amplitudes of about  $15 \text{ m s}^{-1}$  at 91 km height dominate in summer (May-August) with slightly larger meridional than zonal components. This has not been seen in the earlier LF measurements. The phase differences accumulate at values slightly higher than 12 h ( $90^\circ$ ) which refers to a nearly circular polarization. A superposed epoch analysis suggests a relation between baroclinic instability and an amplification of the wave through comparison of vertical shear in the zonal wind as a proxy for instability with the wave amplitudes. The maximum of QTDW amplitude is situated about 10 days after the maximum of shear meaning that the shear amplifies the wave and the wave in turn tends to diminish the source of instability.

Increased winter (November–February) amplitudes have been observed, but with weaker maxima than in summer. A connection to wind shear is not as likely. Instead the 2005–2013 inter-annual variability of winter amplitudes shows some correlation with the 11 year solar cycle, possibly due to a solar cycle dependence of the mesospheric circulation. The

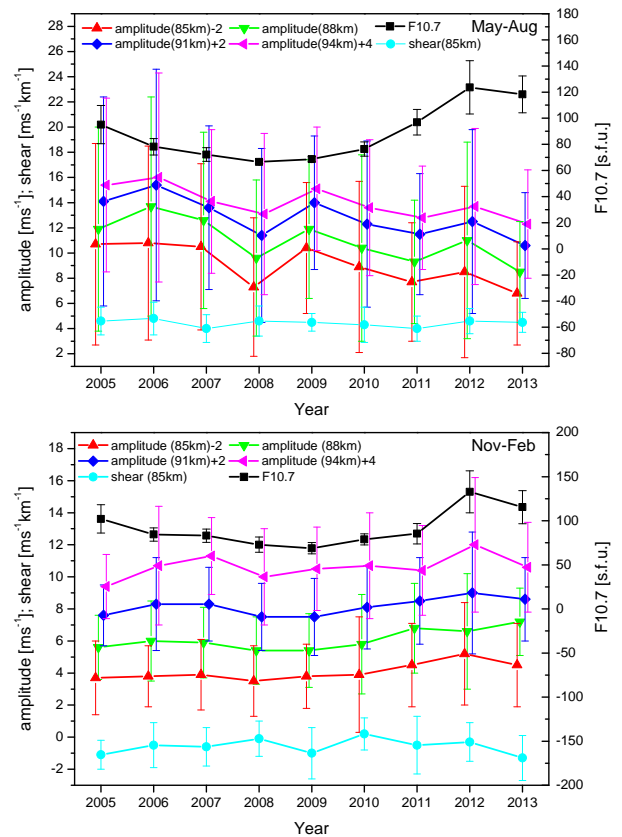


**Figure 6.** Seasonal mean QTDW total amplitudes for summer (May–August, upper panel) and winter (November–February, lower panel), the year refers to the one of the respective January). Error bars denote the standard deviation of the 11 day analyses during one season. Seasonal mean F10.7 solar radio fluxes are added.

correlation coefficient in summer is much lower. Jacobi et al. (2011) show that zonal wind shear and solar cycle are positively correlated, except for the years of solar minimum when correlation turns out to be negative. Since zonal wind shear potentially induces the amplification this may also hold for QTDW amplitudes. Hence, our data are not expected to show good correlation coefficients because they mainly include the deep solar minimum in 2009. Note also that a correlation of QTDW amplitudes and solar proxies using only 9 years of QTDW data will only provide preliminary results, and more substantial conclusions have to be drawn from longer time series. Nevertheless, most of our findings regarding inter-annual variability of the QTDW qualitatively confirm the earlier results by LF measurements.

*Acknowledgements.* F10.7 solar radio flux data have been provided by NGDC through ftp access on [http://ftp.ngdc.noaa.gov/STP/SOLAR\\_DATA/](http://ftp.ngdc.noaa.gov/STP/SOLAR_DATA/).

Edited by: M. Förster  
Reviewed by: two anonymous referees

## References

- Babadshyanov, P. B., Kalchenko, B. V., Kashcheyev, B. L., and Fedynsky, V. V.: Winds in the equatorial lower thermosphere, *Proc. Acad. Sci. USSR*, 208, 1334–1337, 1973 (in Russian).
- Bristow, W. A., Yee, J.-H., Zhu, X., and Greenwald, R. A.: Simultaneous observations of the July 1996 2-day wave event using the Super Dual Auroral Radar Network and the High Resolution Doppler Imager, *J. Geophys. Res.*, 104, 12715–12721, doi:10.1029/1999JA900030, 1999.
- Charney, J. G. and Stern, M. E.: On the Stability of Internal Baroclinic Jets in a Rotating Atmosphere, *J. Atmos. Sci.*, 19, 159–172, doi:10.1175/1520-0469(1962)019<0159:OTSOIB>2.0.CO;2, 1962.
- Craig, R. L. and Elford, W. G.: Observations of the quasi 2day wave near 90 km altitude at Adelaide (35° S), *J. Atmos. Terr. Phys.*, 43, 1051–1056, doi:10.1016/0021-9169(81)90019-2, 1981.
- Ern, M., Preusse, P., Kalisch, S., Kaufmann, M., and Riese, M.: Role of gravity waves in the forcing of the quasi two-day waves in the mesosphere: An observational study, *J. Geophys. Res.*, 118, 3467–3485, doi:10.1029/2012JD018208, 2013.
- Gurubaran, S., Sridharan, S., Ramkumar, T. K., and Rajaram, R.: The mesospheric quasi-2-day wave over Tirunelveli (8.7° N), *J. Atmos. Sol.-Terr. Phys.*, 63, 975–985, doi:10.1016/S1364-6826(01)00016-5, 2001.
- Hocking, W., Fuller, B., and Vandeppeer, B.: Real-time determination of meteor-related parameters utilizing modern digital technology, *J. Atmos. Sol.-Terr. Phys.*, 63, 155–169, doi:10.1016/S1364-6826(00)00138-3, 2001.
- Jacobi, C.: 6 year mean prevailing winds and tides measured by VHF meteor radar over Collm (51.3° N, 13.0° E), *J. Atmos. Sol.-Terr. Phys.*, 78–79, 8–18, doi:10.1016/j.jastp.2011.04.010, 2012.
- Jacobi, C., Schindler, R., and Kürschner, D.: The quasi 2-day wave as seen from DI LF wind measurements over Central Europe (52° N, 15° E) at Collm, *J. Atmos. Sol.-Terr. Phys.*, 59, 1277–1286, doi:10.1016/S1364-6826(96)00170-8, 1997.
- Jacobi, C., Portnyagin, Y. I., Merzlyakov, E. G., Kashcheyev, B. L., Oleynikov, A., Kürschner, D., Mitchell, N. J., Middleton, H., Muller, H. G., and Comley, V. E.: Mesosphere/lower thermosphere wind measurements over Europe in summer 1998, *J. Atmos. Sol.-Terr. Phys.*, 63, 1017–1031, doi:10.1016/S1364-6826(01)00012-8, 2001.
- Jacobi, Ch., Hoffmann, P., Placke, M., and Stober, G.: Some anomalies of mesosphere/lower thermosphere parameters during the recent solar minimum, *Adv. Radio Sci.*, 9, 343–348, doi:10.5194/ars-9-343-2011, 2011.
- Malinga, S. B. and Ruohoniemi, J. M.: The quasi-two-day wave studied using the Northern Hemisphere SuperDARN HF radars, *Ann. Geophys.*, 25, 1767–1778, doi:10.5194/angeo-25-1767-2007, 2007.
- Merzlyakov, E. G. and Jacobi, Ch.: Quasi-two-day wave in an unstable summer atmosphere – some numerical results on excitation and propagation, *Ann. Geophys.*, 22, 1917–1929, doi:10.5194/angeo-22-1917-2004, 2004.
- Muller, H. G.: Long-period meteor wind oscillations, *Phil. T. R. Soc. A*, 271, 585–598, 1972.
- Muller, H. G. and Nelson, L.: A travelling quasi 2-day wave in the meteor region, *J. Atmos. Terr. Phys.*, 40, 761–766, 1978.
- Nozawa, S., Imaida, S., Brekke, A., Hall, C. M., Manson, A., Meek, C., Oyama, S., Dobashi, K., and Fujii, R.: The quasi 2-day wave observed in the polar mesosphere, *J. Geophys. Res.*, 108, 4039, doi:10.1029/2002JD002440, 2003.
- Palo, S. E., Roble, R. G., and Hagan, M. E.: Middle atmosphere effects of the quasi-two-day wave determined from a General Circulation Model, *Earth Planets Space*, 51, 629–647, 1999.
- Pancheva, D. V.: Quasi-2-day wave and tidal variability observed over Ascension Island during January/February 2003, *J. Atmos. Sol.-Terr. Phys.*, 68, 390–407, doi:10.1016/j.jastp.2005.02.028, 2006.
- Pancheva, D. V., Mitchell, N. J., Manson, A. H., Meek, C. E., Jacobi, C., Portnyagin, Y., Merzlyakov, E., Hocking, W. K., MacDougall, J., Singer, W., Igarashi, K., Clark, R. R., Riggan, D. M., Franke, S. J., Kürschner, D. K., Fahrutdinova, A. N., Stepanov, A. M., Kashcheyev, B. L., Oleynikov, A. N., and Muller, H. G.: Variability of the quasi-2-day wave observed in the MLT region during the PSMOS campaign of June–August 1999, *J. Atmos. Sol.-Terr. Phys.*, 66, 539–565, doi:10.1016/j.jastp.2004.01.008, 2004.
- Pendlebury, D.: A simulation of the quasi-two-day wave and its effect on variability of summertime mesopause temperatures, *J. Atmos. Sol.-Terr. Phys.*, 80, 138–151, doi:10.1016/j.jastp.2012.01.006, 2012.
- Pfister, L.: Baroclinic instability of easterly jets with applications to the summer mesosphere, *J. Atmos. Sci.*, 42, 313–330, doi:10.1175/1520-0469(1985)042<0313:BIOEJW>2.0.CO;2, 1985.
- Plumb, R. A.: Baroclinic Instability of the Summer Mesosphere: A Mechanism for the Quasi-Two-Day Wave?, *J. Atmos. Sci.*, 40, 262–270, 1983.
- Plumb, R. A., Vincent, R. A., and Craig, R. L.: The Quasi-Two-Day Wave Event of January 1984 and its Impact on the Mean Mesospheric Circulation, *J. Atmos. Sci.*, 44, 3030–3036, 1987.
- Salby, M. L.: Rossby normal modes in nonuniform background configurations. Part II: Equinox and solstice conditions, *J. Atmos. Sci.*, 38, 1827–1840, 1981a.
- Salby, M. L.: The 2-day wave in the middle atmosphere – observations and theory, *J. Geophys. Res.*, 86, 9654–9660, 1981b.
- Salby, M. L. and Callaghan, P. F.: Seasonal amplification of the 2-day wave: Relationship between normal mode and instability, *J. Atmos. Sci.*, 58, 1858–1869, doi:10.1175/1520-0469(2001)058<1858:SAOTDW>2.0.CO;2, 2001.
- Stober, G., Jacobi, C., Fröhlich, K., and Oberheide, J.: Meteor radar temperatures over Collm (51.3° N, 13° E), *Adv. Space Res.*, 42, 1253–1258, doi:10.1016/j.asr.2007.10.018, 2008.
- Tsuda, T., Kato, S., and Vincent, R. A.: Long period wind oscillations observed by the Kyoto meteor radar and comparison of the quasi-2-day wave with Adelaide HF radar observations, *J. Atmos. Terr. Phys.*, 50, 225–230, doi:10.1016/0021-9169(88)90071-2, 1988.
- Tunbridge, V. M., Sandford, D. J., and Mitchell, N. J.: Zonal wave numbers of the summertime 2 day planetary wave observed in the mesosphere by EOS Aura Microwave Limb Sounder, *J. Geophys. Res.*, 116, D11103, doi:10.1029/2010JD014567, 2011.
- Wu, D. L., Fishbein, E. F., Read, W. G., and Waters, J. W.: Excitation and Evolution of the Quasi 2-Day Wave Observed in UARS/MLS Temperature Measurements, *J. Atmos. Sci.*, 53, 728–738, doi:10.1175/1520-0469(1996)053<0728:EAEOTQ>2.0.CO;2, 1996.